Chapter 5

ERROR ESTIMATES FOR ELLIPTIC PROBLEMS

5.1 Introduction

Having obtained a finite element solution, we would like to be able to estimate the error in that solution and, perhaps, have the analysis program correct itself. Currently, that is a practical option for an elliptic partial differential equation (PDE). Here we will outline the basic method and notation of that class of error estimation. Consider a problem posed by the PDE written as

$$\mathbf{L}\,\phi + Q \;=\; 0 \quad in\ \Omega \tag{5.1}$$

with the essential boundary condition $\phi = \phi_o$ on boundary Γ_ϕ, and a prescribed traction, or flux, $\mathbf{t} = \mathbf{t}_o$ on the boundary Γ_t with $\Gamma = \Gamma_\phi \cup \Gamma_t$. Here $\mathbf{L}$ is a linear differential operator that can usually be written in the symmetric form

$$\mathbf{L} \;\equiv\; D^T\,\mathbf{E}\,D \tag{5.2}$$

where D is a lower order operator and the symmetric constitutive array $\mathbf{E}$ contains material information. The gradient quantities of interest are denoted as

$$\boldsymbol{\varepsilon} \;\equiv\; D\,\phi \tag{5.3}$$

and the flux quantities, $\mathbf{q}$, by some constitutive relation

$$\mathbf{q} \;=\; \pm\,\mathbf{E}\,\boldsymbol{\varepsilon}\,. \tag{5.4}$$

On the boundary, Γ, of Ω we are often interested in a traction, $\mathbf{t}$, defined in terms of the fluxes by

$$\mathbf{t} \;=\; \mathbf{G}\,\mathbf{q} \tag{5.5}$$

where $\mathbf{G}$ is usually defined in terms of the components of the normal vector, $\mathbf{n}$.

For example, in isotropic conduction ϕ is the temperature, Q, in internal volumetric heat source, $\mathbf{E} = k\,\mathbf{I}$, where k is the thermal conductivity, $\mathbf{I}$ is the identity matrix, and D is simply the gradient

$$D^T = \nabla^T = \left[\frac{\partial}{\partial x} \quad \frac{\partial}{\partial y} \quad \frac{\partial}{\partial z} \right]$$

so that **L** becomes the Laplacian, $\mathbf{L} = \nabla^T k \mathbf{I} \nabla$, and for the common case of constant k:

$$\mathbf{L} = k\left(\frac{\partial^2}{\partial x^2} + \frac{\partial^2}{\partial y^2} + \frac{\partial^2}{\partial z^2} \right).$$

In this example $\boldsymbol{\varepsilon}$ is simply the gradient vector

$$\boldsymbol{\varepsilon} = \nabla \phi\,, \quad \boldsymbol{\varepsilon}^T = \left[\frac{\partial \phi}{\partial x} \quad \frac{\partial \phi}{\partial y} \quad \frac{\partial \phi}{\partial z} \right]$$

and the Fourier Law (note the negative sign) defines the heat flux vector

$$\mathbf{q} = -k \mathbf{I} \nabla \phi = -k \nabla \phi, \quad q^T = [q_x \quad q_y \quad q_z].$$

Likewise, for $\mathbf{G} = \mathbf{n}$ the boundary traction is the normal heat flux:

$$\mathbf{t} = \mathbf{n} \cdot \mathbf{q} = q_x n_x + q_y n_y + q_z n_z = q_n = -k\, \partial\phi / \partial n\,.$$

For the one-dimensional case of heat conduction these all reduce to scalars with

$$D = \partial / \partial x\,,\ \mathbf{E} = k\,,\ \boldsymbol{\varepsilon} = \partial\phi / \partial x\,,\ n_x = \pm 1\,,\ \mathbf{q} = q_x = -k\, \partial\phi / \partial x\,,\ \mathbf{t} = \pm q_x\,,$$

and the governing differential equation $\mathbf{L}\phi + Q = 0$ becomes

$$\frac{\partial}{\partial x}\left(k \frac{\partial \phi}{\partial x} \right) + Q = 0$$

in Ω with $\phi = \phi_0$ on Γ_0. While on the boundary Γ_t, the traction $\mathbf{t} = q_n = -k\, n_x\, \partial\phi / \partial x$, and has an assigned value of $q_n = t_0$.

Likewise, for a problem in planar elasticity, $\boldsymbol{\phi}$ and $\boldsymbol{\varepsilon}$ become the displacement vector components $\boldsymbol{\phi} = [u \quad v]^T$ and strain matrix components $\boldsymbol{\varepsilon} = [\varepsilon_x \quad \varepsilon_y \quad \gamma]$, respectively, which are related by the differential operator

$$D = \begin{bmatrix} \dfrac{\partial}{\partial x} & 0 \\ 0 & \dfrac{\partial}{\partial y} \\ \dfrac{\partial}{\partial y} & \dfrac{\partial}{\partial x} \end{bmatrix}.$$

The corresponding fluxes or stress tensor components are $\mathbf{q} = \boldsymbol{\sigma} \equiv [\sigma_x \quad \sigma_y \quad \tau]^T$ which are related to the strains, $\boldsymbol{\varepsilon}$, by the symmetric Hooke's Law "stress-strain" matrix, **E** (without a minus sign). The source **Q** generalizes to the body force vector $\mathbf{Q} = \mathbf{X} = [X_x \quad X_y]^T$. Finally, the surface traction vector $\mathbf{t} = \mathbf{T} = [T_x \quad T_y]$ is related to the surface stresses, $\boldsymbol{\sigma}$, and the components of the outward unit normal vector, **n**, by $\mathbf{T} = \mathbf{G}\boldsymbol{\sigma}$ where

$$\mathbf{G} = \begin{bmatrix} n_x & 0 & n_y \\ 0 & n_y & n_x \end{bmatrix}.$$

In a finite element method we seek a solution $\hat{\phi}$ which, in turn, yields the approximations for the gradient and flux terms, $\hat{\boldsymbol{\varepsilon}}$ and $\hat{\mathbf{q}}$. The standard interpolation gives

$$\phi \approx \hat{\phi} \;=\; \mathbf{N}(x)\,\boldsymbol{\Phi}^e \quad \mathbf{x} \;\; in \;\; \Omega^e \tag{5.6}$$

with a corresponding gradient estimate

$$\boldsymbol{\varepsilon} \approx \hat{\boldsymbol{\varepsilon}} \;=\; D\,\mathbf{N}(\mathbf{x})\,\boldsymbol{\Phi}^e \;\equiv\; \mathbf{B}^e(\mathbf{x})\,\boldsymbol{\Phi}^e \tag{5.7}$$

for $\mathbf{x}$ in Ω^e. Likewise, the flux approximation is

$$\boldsymbol{\sigma} \approx \hat{\boldsymbol{\sigma}} \;=\; \mathbf{E}^e\,\mathbf{B}^e(\mathbf{x})\,\boldsymbol{\Phi}^e\,. \tag{5.8}$$

In this notation the element square matrix and source vector are

$$\mathbf{S}^e \;=\; \int_{\Omega^e} \mathbf{B}^{e^T}\,\mathbf{E}^e\,\mathbf{B}^e\;d\Omega\,, \qquad \mathbf{C}^e_Q \;=\; \int_{\Omega^e} Q^e\,\mathbf{N}^{e^T}\;d\Omega \tag{5.10}$$

and the boundary traction contribution, if any, is

$$\mathbf{C}^b_{q_n} \;=\; \int_{\Gamma^b} q^b_n\,\mathbf{N}^{b^T}\;d\Gamma\,. \tag{5.12}$$

When the element degrees of freedom subset, $\boldsymbol{\Phi}^e \subset \boldsymbol{\Phi}$, have been computed and gathered from substitution into Eqs. 5.6-8, the local errors in an element domain are

$$e_\phi(\mathbf{x}) \;\equiv\; \phi(\mathbf{x}) - \hat{\phi}(\mathbf{x}) \tag{5.13}$$

$$\mathbf{e}_\varepsilon(\mathbf{x}) \;\equiv\; \boldsymbol{\varepsilon}(\mathbf{x}) - \hat{\boldsymbol{\varepsilon}}(\mathbf{x})\,, \qquad \mathbf{x}\;\varepsilon\;\Omega^e \tag{5.14}$$

$$\mathbf{e}_\sigma(\mathbf{x}) \;\equiv\; \boldsymbol{\sigma}(\mathbf{x}) - \hat{\boldsymbol{\sigma}}(\mathbf{x})\,. \tag{5.15}$$

These quantities can be either positive or negative so we will mainly be interested in their absolute value or some normalized measure of them. We will employ integral *norms* for our error measures. On a linear space we can show that a norm has the properties given in Sec. 2.2. In finite elements we often use the *inner product* defined as

$$< u,\; v > \;\equiv\; \int_\Omega u(\mathbf{x})\,v(\mathbf{x})\,d\Omega \tag{5.16}$$

which possesses a natural norm defined as

$$\|\,\phi\,\|^2 \;=\; <\phi,\;\phi> \;=\; \int_\Omega \phi(\mathbf{x})\;\phi(\mathbf{x})\;d\Omega\,. \tag{5.17}$$

This is also called the L_2 *norm*, since it involves the integral of the square of the argument. We wish to minimize the error in the solution, e_ϕ. However, for elliptical problems it can be shown that this corresponds to minimizing the error energy norm, or other related measures. Error estimates commonly employ one of the following norms:

1. The error energy norm $\|\,e\,\|$ defined as

$$\| e \| = \left[\int_\Omega (\boldsymbol{\varepsilon} - \hat{\boldsymbol{\varepsilon}})^T \, \mathbf{E} (\boldsymbol{\varepsilon} - \hat{\boldsymbol{\varepsilon}}) \, d\Omega \right]^{\frac{1}{2}}$$

$$= \left[\int_\Omega (\boldsymbol{\varepsilon} - \hat{\boldsymbol{\varepsilon}})^T \, (\boldsymbol{\sigma} - \hat{\boldsymbol{\sigma}}) \, d\Omega \right]^{\frac{1}{2}} = \left[\int_\Omega \mathbf{e}_\varepsilon^T \, \mathbf{e}_\sigma \, d\Omega \right]^{\frac{1}{2}} \tag{5.18}$$

$$= \left[\int_\Omega (\sigma - \hat{\sigma})^T \, \mathbf{E}^{-1} (\sigma - \hat{\sigma}) \, d\Omega \right]^{\frac{1}{2}} .$$

2. The L_2 flux or stress error norm

$$\| e_\sigma \|_{L_2} = \left[\int_\Omega (\boldsymbol{\sigma} - \hat{\boldsymbol{\sigma}})^T \, (\boldsymbol{\sigma} - \hat{\boldsymbol{\sigma}}) \, d\Omega \right]^{\frac{1}{2}} = \left[\int_\Omega \mathbf{e}_\sigma^T \, \mathbf{e}_\sigma \, d\Omega \right]^{\frac{1}{2}} . \tag{5.19}$$

3. The root mean square stress error, $\Delta\sigma$, given by

$$\Delta\sigma = \| e_\sigma \|_{L_2} / \Omega^{\frac{1}{2}} . \tag{5.20}$$

4. In general, any of these norms is the sum of the corresponding element norms:

$$\| \phi \|^2 = \sum_e \| \phi \|_e^2, \quad \| \phi \|_e^2 = \int_{\Omega^e} \phi^2 \, d\Omega \tag{5.21}$$

and the domain is the union of all of the element domains, $\Omega = \bigcup_e \Omega^e$.

A relative percentage error can be defined as $\eta = 100 \times \| e \| / \| \phi \|$ which represents a weighted root mean square percentage error in the stresses. We can compute a similar estimate relative to the L_2 norms. In most of the literature on the subject of error estimators there is a discussion of the effectivity index, Θ. It is simply the ratio of the estimated error divided by the exact error, $\Theta = \| e \|_{fea} / \| e \|_{exact}$. Usually an

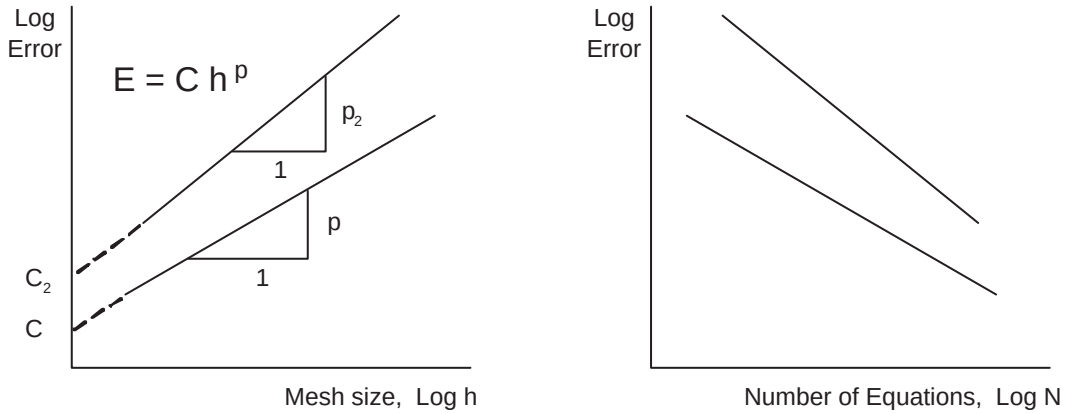

Figure 5.1.1 Asymptotic convergence rates for finite elements

analytical solution is employed to compute the exact error (and to assign the problem source, Q, and boundary conditions, ϕ_0), but sometimes very high precision numerical results are used. Clearly, one should search for methods where the effectivity index is very close to unity. Some methods employ a constant, determined by numerical experiment, to increase their effectivity index to near unity for a specific element type.

From studies in interpolation theory, the finite element approximation is known to converge in the energy norm when $\| e \| \le Ch^p$, for $p > 0$, where h is the distance between nodes on a uniform mesh (the characteristic element length), p is called the rate of convergence. The rate depends on the degree of the polynomial used to approximate ϕ, the order of the highest derivative of ϕ in the weak form, and whether there are local singularities in the domain. The constant, C, is independent of ϕ and will be influenced by the shape of the domain and whether Dirichlet or Neumann boundary conditions are employed. Typically $p = k + 1 - m > 0$ where k is the degree of the highest complete polynomial used in the interpolation and m is the order of the highest derivative of ϕ in the weak form. Remember that simplex elements always use complete polynomials by Lagrangian and Serendipity elements use incomplete polynomials. Note that the above equation for the error would be a straight line plot for a log-log plot of error versus mesh size, as shown in Fig. 5.1.1. In that case the slope of the line is the rate of convergence, p. Such a convergence relation can also be expressed in terms of the number of equations associated with the mesh. In a one-dimensional problem the number of equations, N, is proportional to $1/h$ while in two-dimensions it depends on $1/h^2$, etc. Then the (absolute value of) the slope of the line is the convergence rate divided by the dimension of the space.

5.2 Error Estimates

In general, we do not know the exact strain, $\boldsymbol{\varepsilon}$, or stress values, $\boldsymbol{\sigma}$, in Eqs. (5.3) and (5.4). We do have piecewise continuous estimates for the element strains, $\hat{\boldsymbol{\varepsilon}}$, and stresses, $\hat{\boldsymbol{\sigma}}$, in the element interiors. However, unlike the solution ϕ, these estimates are generally discontinuous between elements. For homogeneous domains (homogeneous $\mathbf{E}$), we expect the exact $\boldsymbol{\varepsilon}$ and $\boldsymbol{\sigma}$ to be continuous. At the interface of two different homogeneous materials ($\mathbf{E}_1$ and $\mathbf{E}_2$), we expect the gradients, $\boldsymbol{\varepsilon}$, to be discontinuous and the fluxes, $\boldsymbol{\sigma}$, to usually be continuous normal to the interface of the two materials (or continuous tangent to the interface in some electromagnetic applications). In most elliptical problems, we expect the normal flux component to be continuous, but the tangential component along the interface may be discontinuous. For some electromagnetic problems the reverse is true for interface flux components. In a homogeneous domain a continuous estimate of $\boldsymbol{\varepsilon}$ and $\boldsymbol{\sigma}$ should be more accurate than would be the piecewise continuous $\hat{\boldsymbol{\varepsilon}}$ and $\hat{\boldsymbol{\sigma}}$. Denote such continuous approximations by $\boldsymbol{\varepsilon}^*$ and $\boldsymbol{\sigma}^*$, respectively. That is, $\hat{\boldsymbol{\sigma}}$ is discontinuous across element boundaries, while the $\boldsymbol{\sigma}^*$ are constructed to be continuous across those boundaries. Then, within an element, the error estimators with good accuracy are

$$\mathbf{e}_\varepsilon \approx \boldsymbol{\varepsilon}^*(\mathbf{x}) - \hat{\boldsymbol{\varepsilon}}(\mathbf{x}), \quad \mathbf{e}_\sigma \approx \boldsymbol{\sigma}^*(\mathbf{x}) - \hat{\boldsymbol{\sigma}}(\mathbf{x}). \tag{5.25}$$

There are various procedures for obtaining nodal values of the strains, ε^*, or stresses, σ^*, that will yield a continuous solution over the domain. Probably the most

common early approach was simply an averaging based on the number and/or size of elements contributing to a node. The continuous nodal stresses were obtained by averaging the values from surrounding elements. However, this simple averaging process does not have any mathematical foundation relative to the original problem and can not be used as part of an effective error estimator. A precise mathematical procedure for computing the nodal values directly was given early in the development of finite element methods by Oden, et al. [8, 15]. However, that "Conjugate Stress" approach required the assembly of element contributions and solving a system of equations equal in size to the number of nodes in the system. More recently for elliptical problems it has been shown that a Super-Convergent Patch (SCP) of elements provides a way to recover accurate continuous nodal fluxes or nodal gradients that can be used in an error estimator. Ainsworth and Oden [3] have carried out an extensive review of the most useful error estimation techniques. They consider both elliptical equations and other classes of problems such as the Navier-Stokes equations.

In Chapter 2 we showed that a patch based averaging process is one way to estimate the value of $\boldsymbol{\sigma}^*$. While we will employ mainly that SCP approach some other methods have proven practical. We will look briefly at hierarchial and flux balancing methods as alternate ways of estimating the error. Then we will follow with a chapter outlining the details of the super-convergence patch averaging and error estimation.

5.3 Hierarchical Error Indicator

Zienkiewicz and Morgan [29] have given a detailed study of how hierarchical interpolation functions can be employed to compute an error estimate. Here we will outline this approach in one-dimension. They define the error norm as

$$\| e \|_E^2 \;=\; -\int_\Omega e\, r\, d\,\Omega$$

where the error is $e = \phi - \hat{\phi}$ and r is the residual error on the interior of the domain

$$L\,\hat{\phi} + q \;=\; r \;\neq\; 0\,.$$

Now we enrich the current approximate solution $\hat{\phi}$ to get a more accurate (higher degree) approximation by adding the next hierarchical bubble function $\phi^* = \hat{\phi} + H_b\, a_b$ where a_b is the next unknown hierarchical degree of freedom. If we take this as representing the correction solution ($\phi \approx \phi^*$), then we have $e^e = H_b^e\, a_b$ and

$$\| e^e \|_E \;=\; a_b \int_{\Omega^e} H_b^{e^T}\, r^e\; d\,\Omega\,.$$

If one can estimate the degree of freedom a_b, then we have an error indicator. If it is the only new dof, and if the hierarchical functions are orthogonal, the new system equilibrium equations are

$$\begin{bmatrix} \mathbf{S} & \mathbf{0} \\ \mathbf{0} & s_{bb} \end{bmatrix} \begin{Bmatrix} \mathbf{a} \\ a_b \end{Bmatrix} = \begin{Bmatrix} \mathbf{C} \\ c_b \end{Bmatrix},$$

where **S** and **C** were the previous system matrices, and s_{bb} and c_b are the new element (and system) stiffness and source terms, respectively. From this diagonal system, we

compute the new term $a_b = c_b / s_{bb}$, that is,

$$c_b = \int_{\Omega^e} H_b^T \, q^e \, d\Omega$$

or from the internal residual definition and the above orthogonality,

$$c_b = \int_{\Omega^e} H_b^T \, (r - L \, \hat{\phi}) \, d\Omega = \int_{\Omega^e} H_b^T \, r^e \, d\Omega .$$

Therefore, this error indicator simplifies to $\| e^e \|_E = a_b \, c_b = c_b^2 / s_{bb}$.

In the following we will use this approach on a one-dimensional sample problem. We will see that the effectivity index is only about one-half, which is unacceptably far from the desired value of unity. While we could introduce a "fudge factor" constant of two, it is wiser to search for a method, like the SCP recovery, that would yield an effectivity index that is always much closer to unity. Consider the Zienkiewicz and Morgan (Z-M) hierarchical error estimator for their Example 8.1 of [29] expanded to consider the local element errors and flux balances. The model problem is

$$- \frac{d^2\phi}{dx^2} + Q = 0 , \qquad x \in]0 , L[, \qquad \phi(0) = 0 , \phi(L) = 0$$

with the exact solution $\phi = Q(x - L) \, x / 2$, so $\phi' = Q(2x - L)/2$. Using the Galerkin approximation:

$$\int_L \phi Q \, dx - \int_L \phi \, \phi_{, xx} \, dx = \int_L \phi Q \, dx - \phi \, \phi_{, x} \Big|_0^L + \int_L \phi_{, x}^2 \, dx = 0$$

or finally

$$\int_L \phi_{, x}^2 \, dx = - \int_L \phi Q \, dx + \phi \, \phi_{, x} \Big|_0^L .$$

Splitting the domain into elements and using our interpolations $\phi_h = \mathbf{H}^e \, \mathbf{u}^e$ this reduces to the matrix form:

$$\sum_e \mathbf{u}^{e^T} \mathbf{K}^e \, \mathbf{u}^e = - \sum_e \mathbf{u}^{e^T} \mathbf{F}_Q^e + u(L) \, \phi_{, x}(L) - u(0) \, \phi_{, x}(0)$$

with the typical element matrices defined (with $\mathbf{E} = \mathbf{I}$) as

$$\mathbf{K}^e = \int_{L^e} \mathbf{H}_{, x}^{e^T} \mathbf{H}_{, x}^e \, dx , \qquad \mathbf{F}_Q^e = \int_{L^e} \mathbf{H}^{e^T} \, Q^e \, dx .$$

For an initial linear interpolation with constant coefficients

$$\mathbf{K}^e = \frac{1}{L^e} \begin{bmatrix} 1 & -1 \\ -1 & 1 \end{bmatrix} , \qquad \mathbf{F}_Q^e = \frac{Q^e L^e}{2} \begin{Bmatrix} 1 \\ 1 \end{Bmatrix} .$$

First, consider a trivial single element solution. By inspection, $L^e = L$ so that

$$\frac{1}{L^e} \begin{bmatrix} 1 & -1 \\ -1 & 1 \end{bmatrix} \begin{Bmatrix} u_1 \\ u_2 \end{Bmatrix} = - \frac{QL^e}{2} \begin{Bmatrix} 1 \\ 1 \end{Bmatrix} + \begin{Bmatrix} - \phi_{, x}(0) \\ + \phi_{, x}(L) \end{Bmatrix}$$

but $u_1 = u_2 = 0$ from the boundary conditions. There are no unknown degrees of freedom to compute so we go directly to the flux recovery and error estimates. Solving for the flux gives $\phi_{,x}(0) = -QL^e/2$ and $\phi_{,x}(L) = QL^e/2$ as the two necessary nodal flux values. Checking we see that a useless solution has still give nodal fluxes that are exact as $L^e \equiv L$. The recovered nodal flux resultants are exact despite the fact that the single element solution is trivial, i.e., $\phi_h = \mathbf{H}^e\,\mathbf{u}^e = \mathbf{H}^e\,\mathbf{O}^e = 0$ (which is exact at nodes). The single element solution is usless in estimating the solution error. In the energy norm the error measure is

$$\| e \|^2 \;=\; -\int_L (\phi - \phi_h)\,(-\phi_{h,x}\,x + Q_h)\,dx \;=\; -\int_L e\,r\,dx$$

where r is the interior residual. To compute an error indicator, we add a quadratic hierarchical term to the linear element so $\phi_h^* = \phi_h + u_3^e\,H_3^e$ where $H_3^e(x) = x(L - x)$ in global space, or $H_3^e(r) = r(1 - r)$ in a local unit coordinate space. The Z-M error indicator is

$$\| e^e \|^2 \;=\; [\int_{L^e} H_3\,r\,dx\,]^2/K_{33}^e\,,\quad K_{33}^e \;=\; \int_{L^e} H_3\,[-H_3^{''}]\,dx$$

is the new hierarchical stiffness term, and $e^e = \phi_h^* - \phi_h$. Here

$$K_{33}^e \;=\; \int_{L^e} r\,(1-r)\,[\,\frac{-1}{L^{e^2}}\,(-2)\,]\,dx \;=\; 1/3L^e$$

and

$$I^e \;=\; \int_{L^e} H_3^e R^e dx \;=\; \int_{L^e} r\,(1-r)\,Q^e dx \;=\; Q^e\,L^e/6$$

so $\| e^e \|^2 = [Q^e L^e/6]^2/(1/3L^e) = Q^{e^2}\,L^{e^3}/12$ which happens to be exact for one element. We now repeat the solution and error indicators for two elements of equal size with $L^e = L/2$. The equilibrium equations are

$$\frac{1}{L^e}\begin{bmatrix} 1 & -1 & 0 \\ -1 & 2 & -1 \\ 0 & -1 & 1 \end{bmatrix}\begin{Bmatrix} u_1 \\ u_2 \\ u_3 \end{Bmatrix} \;=\; -\frac{QL^e}{2}\begin{Bmatrix} 1 \\ 2 \\ 1 \end{Bmatrix} + \begin{Bmatrix} -\phi_{,x}(0) \\ 0 \\ +\phi_{,x}(L) \end{Bmatrix}.$$

Setting $u_1 = 0 = u_3$ the remaining second equation yields $u_2 = -QL^{e^2}/2$, but $L^e = L/2$ so that $u_2 = -QL^2/8$ which is exact. Recovering the fluxes from equilibrium, we first check the global reactions: $\phi_{,x}(0) = -QL^e = -QL/2$, and $\phi_{,x}(L) = +QL/2$, which are both exact. Next, we find the fluxes on each element necessary for local equilibrium:

$$e = 1,\quad \frac{1}{L^e}\begin{bmatrix} 1 & -1 \\ -1 & 1 \end{bmatrix}\begin{Bmatrix} u_1 \\ u_2 \end{Bmatrix} = -\frac{QL^e}{2}\begin{Bmatrix} 1 \\ 1 \end{Bmatrix} + \begin{Bmatrix} -\phi_{,x}(x_1) \\ +\phi_{,x}(x_2) \end{Bmatrix}$$

$$-\frac{1}{L^e}\begin{Bmatrix} -QL^{e^2}/2 \\ +QL^{e^2}/2 \end{Bmatrix} + \frac{QL^e}{2}\begin{Bmatrix} 1 \\ 1 \end{Bmatrix} = QL^e\begin{Bmatrix} 1 \\ 0 \end{Bmatrix} = \begin{Bmatrix} -\phi_{,x}(x_1) \\ +\phi_{,x}(x_2) \end{Bmatrix}$$

which are exact since $L^e = L/2$. Likewise, for $e = 2$,

$$\left\{ \begin{array}{c} -\phi_{,x}(x_2) \\ +\phi_{,x}(x_3) \end{array} \right\} = QL^e \left\{ \begin{array}{c} 0 \\ 1 \end{array} \right\}.$$

The equilibrium of these global and local fluxes are sketched in Fig. 5.6.1. Note that the flux is zero at the symmetry point $(x = x_2)$ as expected. Since Q is a constant, the previously developed element error indicator, $\| e^e \|^2 = Q^{e^2} L^{e^3} / 12$, is still valid for each element and the system error estimate is $\| e \|^2 = \sum_{e=1}^{n_e} = 2 \| e^e \|^2 = Q^{e^2} L^{e^3} / 6$ and since $L^e = L/2$ we get $\| e \|^2 = Q^2 L^3 / 48$ compared to the exact value of $Q^2 L^3/24$. Thus, the total error is underestimated by a factor of two, but the indicator correctly shows each to have the same amount of error.

If we select two unequal elements, we still get exact values for the nodal values and fluxes. That is, if we let $L^e = L/4$ and $L^e = 3L/4$, respectively, we see the results in Fig. 5.6.1. There we note drastic differences in the local errors in each of the two elements. Checking our error indicators we get

$$e = 1 , \qquad \| e^e \|^2 = Q^{e^2} L^{e^3} / 12 = Q^2 L^3 / 768$$

$$e = 2 , \qquad \| e^e \|^2 = Q^2 / 12 \, (3L/4)^3 = 27 Q^2 L^3 / 768 .$$

Clearly, this indicates that the error in the second element is 27 times as large as for that in the first element. Thus, the second element would be selected for refinement. Of course, the total error estimate for the two unequal elements is

$$\sum_{e=1}^{n_e} = 2 \| e^e \|^2 = 28 Q^2 L^3 / 768 , \quad \text{and} \quad \| e \|^2_{exact} = \frac{7}{96} Q^2 L^3 = 56 \, Q^2 L^3 / 768.$$

Refining the second mesh by placing a new node at $x = 3L/4$ gives the results in Fig. 5.6.1. Clearly, the first and third elements have the same indicators

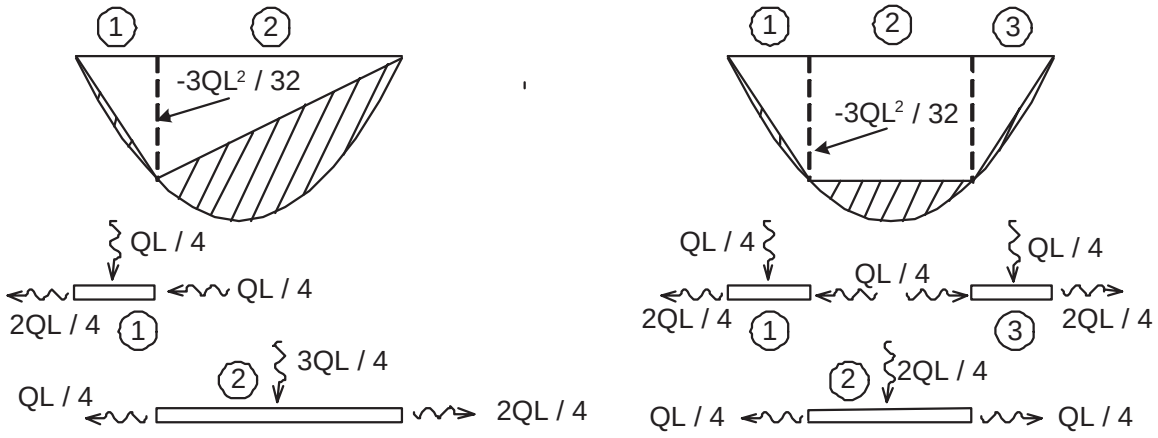

Figure 5.6.1 Sample two and three element solutions, with flux values

$\| e^e \|^2 = Q^2 L^3 / 768$ while the middle element has a value of $\| e^e \|^2 = Q^2 L^3 / 96$. The total error estimate is

$$\| e \|^2 = \sum_{e=1}^{n_e} = 2 \| e^e \|^2 = Q^2 L^3 / 768 [1 + 8 + 1] = 10 Q^2 L^3 / 768 .$$

Therefore, we notice that 10% of the error is in each of the two small elements and the remaining 80% is in the middle element. The exact error and effectivity measures are:

$$\| e \|^2_{exact} = \frac{10}{384} Q^2 L^2 , \qquad \frac{\| e \|^2}{\| e \|^2_{exact}} = 0.5 .$$

Finally, we observe the effects of four equally spaced elements on the error indicators. The system error indicator is the same for all elements and

$$\| e \|^2 = \sum_{e=1}^{n_e} = 4 \| e^e \|^2 = Q^{e^2} L^{e^3} / 3 = Q^2 L^3 / 192,$$

and the exact value is $2 Q^2 L^3 / 192$, and once again we get an effectivity of only 50%. Since we want an error estimator with an effectivity index near unity, this method is not as desirable as the SCP recovery despite correctly giving the relative element error.

5.4 Flux Balancing Error Estimates

Ainsworth and Oden [1−3] have developed a local patch error estimator that is very well justified through detailed functional analysis, is robust, and economical to implement, and gives very accurate local error estimates for any order interpolation functions. That is, it usually produces an effectivity index that is very close to unity and is much more reliable than other methods known to the author. By using a dual variational formulation, they have proved that this estimator provides an *upper bound estimate* of the true error. The Ainsworth-Oden flux balancing method uses a local patch of elements for each master node. A typical patch includes all elements connected, or constrained, to the master node. The goal is to choose a linear averaging function α_{KL} between each pair of adjacent elements, K and L, such that the residual internal error, r, and inter-element gradient jumps, R, are in equilibrium; that is,

$$\int_\Omega r \, d\Omega + \int_\Gamma R \, d\Gamma = 0 . \tag{5.22}$$

They provide a detailed procedure for implementing this method, including pseudo-code for the flux-splitting algorithm. The equilibrium fluxes are used to compute the local error estimator. A summary of the method is as follows:


```
for each master node in patch A do
  begin
    calculate a modified topology matrix, T
    factorize the matrix, L U ≡ T
    for every element e in the patch do
      begin
        calculate mean flux source, b^e
        calculate inter-element weight, ζ_j^e
        assemble patch source, b
      end
    solve for patch constants λ ; L U λ = b
    for every inter-element edge Γ_KL between elements K and L in patch do
      begin
        α_KL = ½ + ( λ_K − λ_L ) / ζ_KL
      end
  end
```

with the topology matrix defined as

$$T_{jk} = \begin{cases} (1 + \text{number of elements in patch}), & \text{if } j = k \\ 0, & \text{if } \Omega^j \text{ and } \Omega^k \text{ are neighbors in patch} \\ 1, & \text{otherwise.} \end{cases}$$

Letting Ψ be a piecewise linear function that is unity at the master node and zero on the patch boundary, the mean source is defined in terms of the model equation

$$-\nabla \cdot (k \nabla u) + \mathbf{b} \cdot \nabla u + c u = f \tag{5.23}$$

as

$$\mathbf{b}^e = L^e(\Psi) - B^e(\hat{u}, \Psi) + \int_{\Gamma^e \setminus \Gamma} \Psi < \mathbf{n}^e \cdot k \nabla \hat{u} >_{\frac{1}{2}} d\Gamma$$

$$L^e(\Psi) = \int_{\Omega^e} f \Psi \, d\Omega + \int_{\Gamma_n} k \frac{\partial u}{\partial n} \Psi \, d\Gamma$$

$$B^e(\hat{u}, \Psi) = \int_{\Omega^e} (k \nabla \hat{u} \cdot \nabla \Psi + \Psi \mathbf{b} \cdot \nabla \hat{u} + c \hat{u} \Psi) \, d\Omega$$

$$< \mathbf{n}^e \cdot k \nabla \hat{u} > = \mathbf{n}^e \cdot \tfrac{1}{2} \left(k^e \nabla \hat{u} \Big|_{\Omega^e} + k^j \nabla \hat{u} \Big|_{\Omega^j} \right)$$

and the inter-element weight is

$$\zeta_j^e = -\int_{\Gamma_j^e} \Psi \left(\mathbf{n}^e \cdot k^e \nabla \hat{u} \Big|_{\Omega^e} + \mathbf{n}^j \cdot k^j \nabla \hat{u} \Big|_{\Omega^j} \right) d\Gamma .$$

The actual flux-splitting function on the boundary between nodes K and L is

$$\alpha_{KL}(s) = \sum_{A} \alpha_{KL}\ \Psi(s)$$

where the sum has taken over all patches containing edge *KL* (and a non-zero Ψ). Once the fluxes are in equilibrium, the error, $e = u - \hat{u}$, is bounded above by the norm

$$\| e \|^2 \le \frac{1}{\beta^2} \sum_{e=1}^{n_e} \| \phi^e \|^2$$

where $\beta > 0$ is a constant depending on the norm selected ($\beta = 1$ for the standard energy norm), and ϕ is obtained by solving the element local Neumann problem

$$a^e(\phi, w) = L^e(w) - B^e(\hat{u}, w) + \tag{5.24}$$
$$+ \int_{\Gamma^e} w\, \mathbf{n}^e \cdot \left[(1 - \alpha_{KL}(s))\, k^e \nabla \hat{u} \Big|_{\Omega^e} + \alpha_{KL}(s)\, k^j \nabla \hat{u} \Big|_{\Omega^f} \right] d\Gamma .$$

The examples by Ainsworth and Oden show this procedure to be accurate and economical. The effectivity index, Θ, is usually very near unity as desired, and is usually above 0.9 for even crude initial mesh calculations. While this is also a recommended method, we choose to implement SCP recovery due to its simplicity.

5.5 Element Adaptivity

Upon completing the loop over all elements we have the element norms, the element volume, the system norms,

$$\|\mathbf{e}\|^2 = \sum_{e}^{n_e} \|\mathbf{e}^e\|^2 , \tag{5.25}$$

and the system volume. The allowed error energy is obtained from the product of the strain energy norm and the user input value of the allowed percentage error, η (keyword input value *scp_allow_error_*%). That number is used, in turn, to evaluate two allowed error densities in dividing by the square root of the number of elements and the square root of the volume to yield mean element and volumetric references, respectively. One of these reference values will be used to rank the relative error measures in each element. The system norm values are printed along with the two allowable reference values for the energy error and the system volume. For each element we will list the element error norm, its percentage of the strain energy norm, and a refinement parameter for that element. The element error energy norms are summed to get the total energy in the error to compare to the total strain energy norm and the allowed percentage of error. Here, the refinement parameter is based on the volumetric error density, so for element j the refinement parameter is

$$\xi_j = (\|\mathbf{e}_j\| / \sqrt{\Omega_j}) / (\eta \|\mathbf{e}\| / \sqrt{\Omega})$$

or

$$\xi_j = \frac{\|\mathbf{e}_j\|}{\eta \|\mathbf{e}\|} \left(\frac{\Omega}{\Omega_j} \right)^{\frac{1}{2}} . \tag{5.26}$$

Here it is informative to note that for a uniform mesh all the n_e element volumes are constant with a value of

$$\Omega_j = \Omega / n_e$$

and the refinement indicator becomes the same as originally employed by Zienkiewicz and Zhu, namely:

$$\xi_j = \frac{\|\mathbf{e}_j\|}{\eta \|\mathbf{e}\| \sqrt{n_e}} . \tag{5.27}$$

By combining such an indicator with interpolation error analysis, one can predict the desired element size or polynomial degree. For each element, i, we define the ratio ξ to indicate needed refinement when $\xi_i > 1$ and de-refinement when $\xi_i < 1$.

5.6 H-Adaptivity

The refinement indicator of Eq. 5.27 is the ratio of the current estimated error in an element to that desired in the element. From interpolation theory the asymptotic convergence rates for an element in a uniform mesh is $\| e \| = Ch^p$, for $p > 0$, where h is the the characteristic element length (distance between nodes), p is the degree of the polynomial, and C is a constant that depends on the shape of the domain and the boundary conditions (Dirichlet versus Neumann). In h-adaptivity we hold the polynomial degree, p, constant and seek a new element size, say h_{new}. Thus, we can also view the refinement indicator as related to the current and new sizes, namely for the j-th element:

$$\xi_j = \frac{Ch_j^p}{Ch_{new}^p} . \tag{5.28}$$

Cancelling the problem constant, C, and factoring the out the polynomial order, p, the new element size should be

$$h_{new} = h_j / \xi_j^{1/p} . \tag{5.29}$$

It should be noted that some analysts like to normalize the asympotic rate by dividing the element size by its initial size. That is, after a few iterations they employ $(h / h_0)^p$ where h_0 was the element size in the original mesh.

The relation in Eq. 5.29 is used to output a sequential list of desired element sizes to be utilized as input by an automatic mesh generator. It could be arbitrarily associated with the element centroid. Here it is output at each current node using the average value of all the elements connected to the node. Huang and Usmani provide such an automatic mesh generator for two-dimensional applications [11]. A modified version of their source code was used for several of the examples given herein.

5.7 P-Adaptivity

In p-adaptivity it is less clear how to proceed and several hueristic approaches have been used. It is clear that the new polynomial degree must be an integer. The change in degree should be small (1 or 2) because higher order elements are expensive. Also numerical studies show that the nature of the error is different in even and odd order polynomials. The interior error (measured well by the SCP) is more important in even polynomials, while the interface flux jump error is more important in odd order elements.

Thus, one could simply assume the element size will be constant and note which integer increase in p would give a refinement indicator slightly smaller that the one obtained from the error estimator. In global p-refinements typically use the largest integer found in this way (but limiting the new polynomial to ≤ 6). However, that can be very expensive.

There is another empirical equation for estimating the new polynomial degree. If one assumes Lagrange interpolation and views h as the distance between nodes then a real number estimate of the new degree is

$$p_{Est} = p \times \xi_j^{1/p} \tag{5.30}$$

which would have to rounded to an integer value, p_{new}. Typical results from this estimate are illustrated below:

ξ	p_{old}	$\xi^{1/p_{old}}$	p_{Est}	Operation	p_{new}
4.00	2	2.00	4.0	Enrich	4
1.00	2	1.00	2.0	No Change	2
0.50	2	0.71	1.4	No Change	2
0.05	2	0.22	0.45	Degrade	1
4.00	3	1.59	4.76	Enrich	5
2.00	3	1.26	3.78	Enrich	4
0.50	3	0.79	2.38	Degrade	2

Clearly, arbitrary rules govern how to round the estimated p in the fourth column. The third line value of 1.4 might just have easily been thought of as a degrade to a linear polynomial ($p_{new} = 1$).

5.8 HP-Adaptivity

It has been proved (see Ainsworth and Oden [3] for example) that an hp-adaptive system gives the optimal convergence (maximum accuracy for a given number of equations). However, its programming is difficult and requires careful planning of the data base structure. In an hp-adaptive solution one needs to pick which item to change first. Since p changes are relative expensive and must be limited to integers it may be best to select p_{new} first and to restrict the change in degree, say n to 0 or $+-1$. Then due to the integer choice on p some of the estimated refinement (or de-refinement) still needs to occur by also selecting a new mesh size. We can envision the refinement indicator as having two contributions, $\xi = \xi_p \times \xi_h$. If the new integer degree, $(p + n)$, was based on the current element size then the now known numerical value $\xi_p = h^p / h^{(p+n)}$ can be used to get the needed remaining spatial refinement indicator , ξ_h. Note that the product relation is

$$\xi = \frac{h^p}{h_{new}^{(p+n)}} = \frac{h^p}{h^{(p+n)}} \times \frac{h^{(p+n)}}{h_{new}^{(p+n)}} = \xi_p \times \xi_h \tag{5.31}$$

which with ξ and ξ_p known simplifies to

$$\xi_h = (\xi / \xi_p) = (h / h_{new})^{(p+n)}$$

or finally

$$h_{new} = h / \xi_h^{1/(p+n)} . \tag{5.32}$$

Even with these rough estimates of desired changes one may need other rules to assure that the mesh size and local degree do not change rapidly from one solution iteration to the next, or oscillate between large and small values.

5.9 Exercises

1. A four element model of our previous example differential equation, $u,xx + u + x = 0$, $u(0) = 0 = u(1)$ yields the exact and finite element solution as shown in Prob. 5.1a and the true flux is shown in Prob. 5.1b. The finite element flux estimates in the elements consists of the four constant steps listed above. Obtain a nodal continuous flux estimate by using element based patches (four in total). Show the estimated (eyeball) linear fit on each patch. For each patch use a unique symbol to show the interpolated nodal flux values. At each original mesh node average the nodal flux values from all patches. Plot a piecewise linear curve through those average flux values and compare it to the exact flux curve in Prob. 5.1b. Utilize those numerical results, for the two-noded linear element (L2).

2. Resolve the example in Chapter 2 for $k\, d^2\phi / dx^2 + Q = 0$ with $\phi(L) = \phi_L$, and $k\, d\phi / dx\,(0) = q_0$ using a four element model. Plot the results compared to the exact solution. Obtain the gradient estimate in each element at its centroid, and plot it against the true gradient. Obtain a nodal continuous flux estimate by using element based

```
*** OUTPUT OF RESULTS AND EXACT VALUES IN NODAL ORDER ***  ! 1
NODE,  X-Coord,    DOF_1,      EXACT1,                    ! 2
   1  0.0000E+00  0.0000E+00  0.0000E+00                   ! 3
   2  2.5000E-01  4.3758E-02  4.4014E-02                   ! 4
   3  5.0000E-01  6.9345E-02  6.9747E-02                   ! 5
   4  7.5000E-01  5.9715E-02  6.0056E-02                   ! 6
   5  1.0000E+00  0.0000E+00 -2.2829E-10                   ! 7
                                                           ! 8
*** FE AND EXACT FLUX COMPONENTS AT INTEGRATION POINTS *** ! 9
ELEMENT, PT,  X-Coord,    FX_1,     EX_1,                 !10
       1  1  5.283E-02  1.750E-01  1.867E-01               !11
       1  2  1.972E-01  1.750E-01  1.654E-01               !12
ELEMENT, PT,  X-Coord,    FX_1,     EX_1,                 !13
       2  1  3.028E-01  1.023E-01  1.343E-01               !14
       2  2  4.472E-01  1.023E-01  7.155E-02               !15
ELEMENT, PT,  X-Coord,    FX_1,     EX_1,                 !16
       3  1  5.528E-01 -3.852E-02  1.137E-02               !17
       3  2  6.972E-01 -3.852E-02 -8.890E-02               !18
ELEMENT, PT,  X-Coord,    FX_1,     EX_1,                 !19
       4  1  8.028E-01 -2.389E-01 -1.745E-01               !20
       4  2  9.472E-01 -2.389E-01 -3.060E-01               !21
```

P5.1 Four linear element results

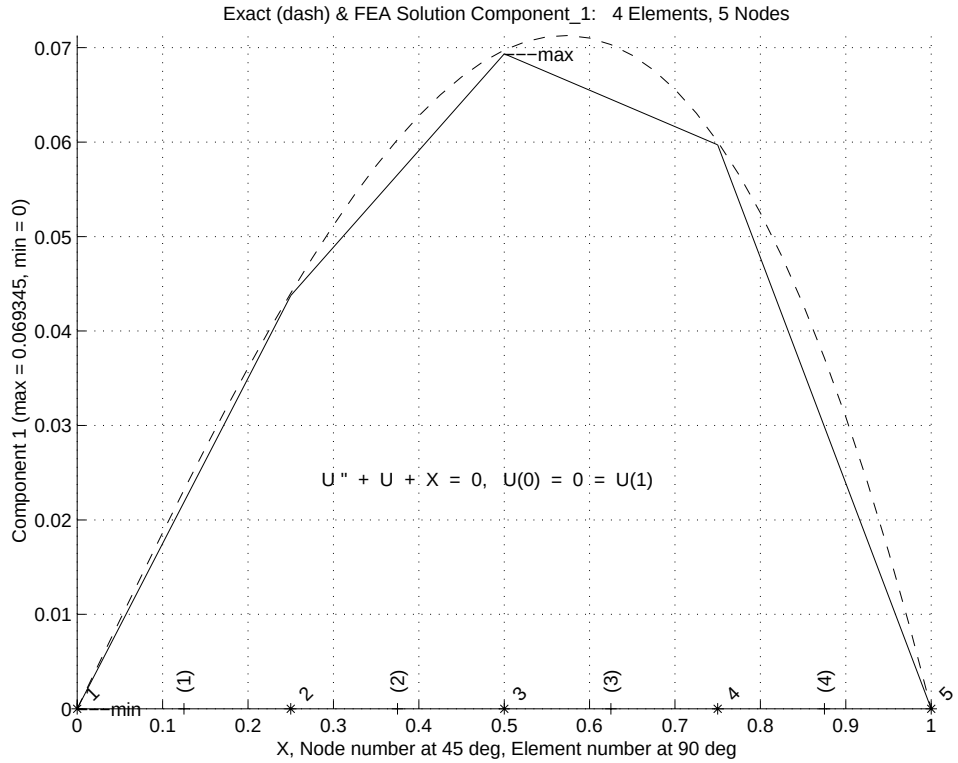

Prob. 5.1a Exact and FEA solution of ODE

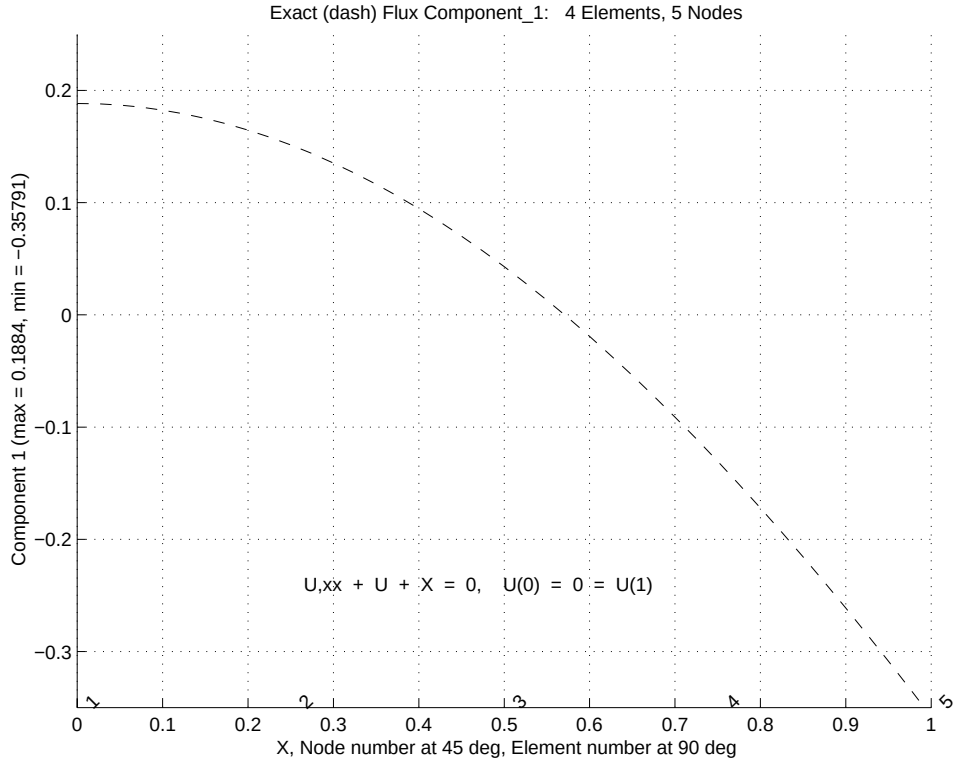

Prob. 5.1b Exact flux for ODE

patches (four in total). Show the estimated (eyeball) linear fit on each patch. For each patch use a unique symbol to show the interpolated nodal flux values. At each original mesh node average the nodal flux values from all patches. Plot a piecewise linear curve through those average flux values and compare it to the exact gradient. Use a) $L = 1$, $k = 1$, $q_0 = 2$, $\phi_L = 1$, and $Q = Q_0 = 1$ so that the exact solution is given by $k\,\phi(x) = k\,\phi_L + q_0(x - L) + Q_0\,(L^2 - x^2)/2$, b) $L = 1$, $k = 1$, $q_0 = 1/12$, $\phi_L = 0$, and $Q = x^2$ so the exact solution is $\phi(x) = (x - x^4)/12$.

5.10 Bibliography

[1] Ainsworth, M. and Oden, J.T., "A Procedure for *a Posteriori* Error Estimation for *h-p* Finite Element Methods," *Comp. Meth. Appl. Mech. Eng.*, **101**, pp. 73−96 (1992).

[2] Ainsworth, M. and Oden, J.T., "A Unified Approach to *a Posteriori* Error Estimation Based on Element Residual Methods," *Numer. Math.*, **65**, pp. 23−50 (1993).

[3] Ainsworth, M. and Oden, J.T., *A Posteriori Error Estimation in Finite Element Analysis*, New York: John Wiley (2000).

[4] Babuska, I., Strouboulis, T., and Upadhyay, C.S., "A Model Study of the Quality of *a Posteriori* Error Estimators for Finite Element Solutions of Linear Elliptic Problems, with Particular Reference to the Behavior near the Boundary," *Int. J. Num. Meth. Eng.*, **40**, pp. 2521−2577 (1997).

[5] Babuska, I. and Strouboulis, T., *The Finite Element Method and its Reliability*, Oxford: Oxford University Press (2001).

[6] Barnhill, R.E. and Whiteman, J.R., "Error Analysis of Finite Element Methods with Triangles for Elliptic Boundary Value Problems," in *The Mathematics of Finite Elements and Applications*, ed. J.R. Whiteman, London: Academic Press (1973).

[7] Blacker, T. and Belytschko, T., "Superconvergent Patch Recovery with Equilibrium and Conjoint Interpolant Enhancements," *Int. J. Num. Meth. Eng.*, **37**, pp. 517−536 (1995).

[8] Brauchli, H.J. and Oden, J.T., "On the Calculation of Consistent Stress Distribution in Finite Element Applications," *Int. J. Num. Meth. Eng.*, **3**, pp. 317−325 (1971).

[9] Ciarlet, P.G., *The Finite Element Method for Elliptical Problems*, Philadelphia, PA: SIAM (2002).

[10] Cook, R.D., Malkus, D.S., Plesha, N.E., and Witt, R.J., *Concepts and Applications of Finite Element Analysis*, New York: John Wiley (2002).

[11] Huang, H.C. and Usmani, A.S., in *Finite Element Analysis for Heat Transfer*, London: Springer-Verlag (1994).

[12] Kelly, D.W., "The Self Equilibration of Residuals and Complementary *a Posteriori* Error Estimates in the Finite Element Method," *Int. J. Num. Meth. Eng.*, **20**, pp. 1491−1506 (1984).

[13] Krizek, M., Neittaanmaki, P., and Stenberg, R., *Finite Element Methods: Superconvergence, Post-Processing and a Posteriori Estimates*, New York: Marcel Dekker, Inc. (1998).
[14] Ladeveze, D. and Leguillon, D., "Error Estimate Procedure in the Finite Element Method and Applications," *SIAM J. Num. Anal.*, **20**(3), pp. 485−509 (1983).
[15] Oden, J.T., *Finite Elements of Nonlinear Continua*, New York: McGraw-Hill (1972).
[16] Oden, J.T., *Applied Functional Analysis*, Englewood Cliffs: Prentice-Hall (1979).
[17] Oden, J.T., "The Best FEM," *Finite Elements in Analysis and Design*, **7**, pp. 103−114 (1990).
[18] Szabo, B. and Babuska, I., *Finite Element Analysis*, New York: John Wiley (1991).
[19] Wiberg, N-E., Abdulwahab, F., and Ziukas, S., "Enhanced Superconvergent Patch Recovery Incorporating Equilibrium and Boundary Conditions," *Int. J. Num. Meth. Eng.*, **37**, pp. 3417−3440 (1994).
[20] Wiberg, N-E., Abdulwahab, F., and Ziukas, S., "Improved Element Stresses for Node and Element Patches Using Superconvergent Patch Recovery," *Com. Num. Meth. Eng.*, **11**, pp. 619−627 (1995).
[21] Wiberg, N-E., "Superconvergent Patch Recovery − A Key to Quality Assessed FE Solutions," *Adv. Eng. Software*, **28**, pp. 85−95 (1997).
[22] Zhang, Z. and Zhu, J.Z., "Analysis of the Superconvergent Patch Recovery Technique and *a posteriori* Error Estimator in the Finite Element Method (I)," *Computer Methods in Applied Mechanics and Engineering*, **123**, pp. 173−187 (1995).
[23] Zhang, Z., "Ultraconvergence of the Patch Recovery Technique," *Math. Comp.*, **65**, pp. 1431−1437 (1996).
[24] Zhang, Z., "Derivative Superconvergence Points in Finite Element Solutions of Poisson's Equation for the Serendipity and Intermediate Families − A Theoretical Justification," *Math. Comp.*, **67**, pp. 541−552 (1998).
[25] Zhang, Z. and Zhu, J.Z., "Analysis of the Superconvergent Patch Recovery Technique and *a posteriori* Error Estimator in the Finite Element Method (II)," *Computer Methods in Applied Mechanics and Engineering*, **163**, pp. 159−170 (1998).
[26] Zhang, Z., "Ultraconvergence of the Patch Recovery Technique II, with Graph," *Math. Comp.*, **69**, pp. 141−158 (2000).
[27] Zhu, J.Z. and Zienkiewicz, O.C., "Superconvergence Recovery Techniques and *A Posteriori* Error Estimators," *Int. J. Num. Meth. Eng.*, **30**, pp. 1321−1339 (1990).
[28] Zhu, J.Z., "Derivative Recovery Techniques and *a Posteriori* Error Estimation in the Finite Element," *SIAM J. Appl. Num. Anal.*, **N**, pp. **nn−nnn** (1992).
[29] Zienkiewicz, O.C. and Morgan, K., *Finite Elements and Approximation*, Chichester: John Wiley (1983).

[30] Zienkiewicz, O.C. and Zhu, J.Z., "A Simple Error Estimator and Adaptive Procedure for Practical Engineering Analysis," *Int. J. Num. Meth. Eng.*, **24**, pp. 337−357 (1987).

[31] Zienkiewicz, O.C., Kelley, D.W., Gago, J., and Babuska, I., "Hierarchal Finite Element Approaches Error Estimates and Adaptive Refinement," pp. 313−346 in *The Mathematics of Finite Elements and Applications, VI*, ed. J.R. Whiteman, London: Academic Press (1988).

[32] Zienkiewicz, O.C., Zhu, J.Z., Craig, A.W., and Ainsworth, M., "Simple and Practical Error Estimation and Adaptivity," pp. 100−114 in *Adaptive Methods for Partial Differential Equations*, ed. J.E. Flaherty et al., SIAM (1989).

[33] Zienkiewicz, O.C. and Zhu, J.Z., "Superconvergent Patch Recovery Techniques and Adaptive Finite Element Refinement," *Comp. Meth. Appl. Mech. Eng.*, **101**, pp. 207−224 (1992).

[34] Zienkiewicz, O.C. and Zhu, J.Z., "The Superconvergent Patch Recovery and *a Posteriori* Error Estimates. Part 2: Error Estimates and Adaptivity," *Int. J. Num. Meth. Eng.*, **33**, pp. 1365−1382 (1992).

